THE JOURNAL OF BIOLOGICAL CHEMISTRY
Vol. 272, No. 36, Issue of September 5, pp. 22531–22537, 1997
Printed in U.S.A.

Differential Targeting of Nicotinic Acetylcholine Receptors by Novel αA-Conotoxins*

(Received for publication, January 31, 1997, and in revised form, May 12, 1997)

Richard Jacobsen‡, Doju Yoshikami‡, Michael Ellison‡, Jennifer Martinez‡, William R. Gray‡, G. Edward Cartier‡, Ki-Joon Shon§, Duncan R. Groebe¶, Stewart N. Abramson¶, Baldomero M. Olivera‡, and J. Michael McIntosh‡‖****

From the Departments of ‡Biology and ‖Psychiatry, University of Utah, Salt Lake City, Utah 84112, the §Department of Physiology and Biophysics, Case Western Reserve University, Cleveland, Ohio 44106, and the ¶Department of Pharmacology, University of Pittsburgh, Pittsburgh, Pennsylvania 15261

We describe the isolation and characterization of two peptide toxins from *Conus ermineus* venom targeted to nicotinic acetylcholine receptors (nAChRs). The peptide structures have been confirmed by mass spectrometry and chemical synthesis. In contrast to the 12–18 residue, 4 Cys-containing α-conotoxins, the new toxins have 30 residues and 6 Cys residues. The toxins, named αA-conotoxins EIVA and EIVB, block both *Torpedo* and mouse α1-containing muscle subtype nAChRs expressed in *Xenopus* oocytes at low nanomolar concentrations. In contrast to α-bungarotoxin, αA-EIVA is inactive at α7-containing nAChRs even at micromolar concentrations. In this regard, αA-EIVA is similar to the previously described α-conotoxins (*e.g.* α-MI and α-GI) which also selectively target α1- *versus* α7-containing nAChRs. However, α-MI and α-GI discriminate between the α/δ *versus* α/γ subunit interfaces of the mouse muscle nAChR with 10,000-fold selectivity. In contrast, αA-conotoxin EIVA blocks both the α/γ site and α/δ site with equally high affinity but with distinct kinetics. The αA-conotoxins thus represent novel probes for the α/γ as well as the α/δ binding sites of the nAChR.

The carnivorous cone snails (genus *Conus*) comprise 500 species that specialize on a variety of prey, including fish. There are ~50–70 different fish-hunting *Conus* species which use venom as the primary weapon for immobilizing prey. Their venoms are extremely complex, and each *Conus* species has its own distinct complement of biologically active venom peptides. Nevertheless, all fish-hunting *Conus* venoms examined so far inhibit neuromuscular transmission. In all cases, one major molecular target involved in this inhibition is the nicotinic acetylcholine receptor (nAChR)[1] at the neuromuscular junction. Thus, all fish-hunting cone snail venoms appear to contain a major venom peptide which, like the snake toxin α-bungarotoxin, potently inhibits the postsynaptic nAChR by competitively blocking the acetylcholine (ACh) binding site.

Despite this common mechanism of action, there are considerable differences in the structures of the nAChR-antagonist peptides in the venoms of various fish-hunting cone snails. The major family of such peptides identified so far are the α-conotoxins, which have been characterized from several species of Indo-Pacific fish-hunting cone snails (1). Recently, a peptide which is a competitive nAChR antagonist was purified and characterized from the Eastern Pacific piscivorous *Conus* species, *Conus purpurascens* (the purple cone) (2). This peptide, αA-PIVA, has a disulfide framework entirely different from all other competitive nAChR antagonists from *Conus*. The peptide has three disulfide bonds instead of the two usually found in α-conotoxins. Furthermore, no obvious homology is detected between α- and αA-conotoxins when their sequences are aligned. Thus, the isolation of αA-PIVA suggests that there may be two major groups of competitive nicotinic antagonists in the venom of fish-hunting cone snails, the α- and the αA-conotoxins.

Perhaps the most closely related fish-hunting *Conus* species to *C. purpurascens* is the "turtle" cone, *Conus ermineus*, which is found throughout the tropical Atlantic (see Fig. 1). However, the first nAChR antagonist which we purified from *C. ermineus* venom was not homologous to αA-PIVA, but was instead a highly divergent α-conotoxin, α-EI (3). In this report, we demonstrate that in addition to α-EI, the venom of *C. ermineus* contains two other nicotinic antagonists, which are αA-conotoxins by virtue of their structural homology to αA-PIVA.

The discovery of these two peptides, αA-conotoxins EIVA and EIVB, expands the membership of the αA-conotoxin family and provides initial structure-function information which will be useful for studies using this family of nicotinic antagonists. The three-dimensional structures of α-conotoxins GI (4) and PnIA are known (5), and that of the first αA-conotoxin was recently solved.[2] Thus, the α- and αA-conotoxins now provide two sets of ligands of known three-dimensional structure that can be used to probe the ligand binding sites of nAChRs in vertebrate muscle. We demonstrate here that the new αA-conotoxins have a selectivity profile which differs from both the α-conotoxins and α-bungarotoxin.

EXPERIMENTAL PROCEDURES

Materials—Crude venom was obtained from milkings of *C. ermineus* kept in aquaria. The venom was stored at −70 °C until used. Trifluoroacetic acid (sequencing grade) was from Aldrich, acetonitrile (UV grade) was from Baxter, and [^{125}]α-BTX was from NEN Life Science Products.

Venom Preparation—Individual milkings of *C. ermineus* venom (2, 3) collected from 10 snails were pooled (final volume 1.5 ml) and concentrated by lyophilization to 0.5 ml. The concentrate was mixed with 3 ml of 0.1% trifluoroacetic acid just prior to application onto an HPLC column.

Goldfish Bioassay—Purification of the paralytic toxin was monitored by injecting fractions into goldfish as described previously (3).

* This work was supported primarily by United States Public Health Service Grant PO1 GM48677. The costs of publication of this article were defrayed in part by the payment of page charges. This article must therefore be hereby marked "*advertisement*" in accordance with 18 U.S.C. Section 1734 solely to indicate this fact.

** Supported by Grant MH53631 and National Institutes of Health Scientist Development Award for Clinicians K20 MH00929. To whom correspondence should be addressed: University of Utah, 201 South Biology, Salt Lake City, UT 84112. Tel.: 801-585-3622; Fax: 801-585-5010; E-mail mcintosh@bioscience.utah.edu.

[1] The abbreviations used are: nAChR, nicotinic acetylcholine receptor; BTX, bungarotoxin; HPLC, high performance liquid chromatography.

[2] Han, K. H., Hwang, K. J., Kim, S. K., Gray, W. R., Olivera, B. M., Rivier, J., and Shon, K. J. (1997) *Biochemistry* **36,** 1669–1677.

FIG. 1. ***C. ermineus* and other *Conus* species.** *A*, three specimens of the turtle cone, *C. ermineus*. *B*, the magus cone, *C. magus*. *C*, the purple cone, *C. purpurascens*. Note that from the shell characters, *C. ermineus* and *C. purpurascens* appear to be more closely related to each other than they are to *C. magus*. *Bar* = 1 cm.

HPLC Purification—The HPLC apparatus consisted of HPXL pumps and either a Dynamax model UVI or UV-DII detector (Rainin, Woburn, MA). All columns were also from Rainin. For isolation of peptide from venom and all subsequent purifications, buffer A consisted of 0.1% trifluoroacetic acid, and buffer B was 0.092% trifluoroacetic acid, 60% acetonitrile. Initial purification of αA-EIVA from milked venom was accomplished using a semipreparative C_{18} Vydac column (10 mm × 25 cm, 5-μm particle size), with a flow rate of 5.0 ml/min. Subsequent purification steps of αA-EIVA utilized an analytical C_{18} Microsorb or Vydac column (4.6 mm × 25 cm, 5-μm particle size) with a flow rate of 1.0 ml/min.

Sequence Analysis—Purified peptides were reduced by dithiothreitol, alkylated with 4-vinylpyridine, and HPLC-purified by previously described methods (3). Sequencing was performed by an Applied Biosystems Model 477A protein sequencer at the Protein/DNA Core Facility at the University of Utah Cancer Center.

Mass Spectrometry—Liquid secondary ionization mass spectra were measured using a Jeol HX110 (JEOL, Tokyo, Japan) double-focusing mass spectrometer operated at a 10-kV accelerating voltage and a nominal resolution of 3000. The sample (in 0.1% aqueous trifluoroacetic acid and 25% acetonitrile) was mixed in a glycerol/3-nitrobenzyl alcohol matrix (1:1) and analyzed with an electric field/accelerating voltage scan over a narrow mass range. The mass accuracy of the HX110 instrument under these conditions was typically better than 50 ppm.

Solid-phase Peptide Synthesis—Peptides were built on Rink amide resin using standard Fmoc (*N*-(9-fluorenyl)methoxycarbonyl) chemistry on an ABI Model 431A peptide synthesizer. Coupling was carried out using equimolar amounts of amino acid derivative, dicyclohexylcarbodiimide and 1-hydroxybenzotriazole. Amino acid side chains were protected as follows: Asp, *trans*-4-hydroxyproline (Hyp), Ser, Thr, Tyr (*tert*-butyl); Cys, His (*trityl*); Lys (*tert*-butoxycarbonyl) and Arg (pentamethylchromansulfonyl).

Linear peptides were released from resin (typically 100 mg), deprotected, and precipitated as detailed previously (7, 8). After precipitation, pelleted peptides were readily soluble in 60% acetonitrile, 0.092% trifluoroacetic acid in H_20. Peptides were purified by HPLC using Vydac C_{18} columns and eluted with buffers containing 0.1% trifluoroacetic acid in H_20 (buffer A) and 60% acetonitrile, 0.092% trifluoroacetic acid in H_20 (buffer B). Typically a linear gradient of 10–50% buffer B over 40 min was used.

The linear peptides were first purified on a preparative HPLC column (22 mm × 25 cm, 10-μm particle size, 300-Å pore size, flow 20 ml/min). Following this, disulfide bonds were formed by oxidation with glutathione. Ten ml of 100 mM I_2 in MeOH was added to 100 ml of 80 mM glutathione in H_20 to make a stock solution of 40 mM reduced (GSH) and 20 mM oxidized (GSSG) glutathione. This solution was added to HPLC effluent containing linear peptide to make a final concentration of 1 mM GSH, 0.5 mM GSSG. The pH was adjusted to 7.5 using dry Tris base or 0.75 M dibasic sodium phosphate buffer (pH 7.7), and the solution was incubated ~20 h at room temperature. The resulting mixture of oxidized peptides potentially contained 15 isomers with different disulfide arrangements. The major product was purified on a preparative column followed by isocratic purification at 21% buffer B on a semipreparative column (10 mm x 25 cm, 5-μm particle size, 300-Å pore size, flow 3 ml/min). Based on HPLC co-elution experiments and biological activity in goldfish, it was determined that both αA-EIVA and αA-EIVB are the major products under the oxidation conditions used.

Electrophysiology—cRNA encoding nAChR subunits was prepared and injected into *Xenopus* oocytes as described previously (8). Oocytes were injected 1–2 days after harvesting and used for voltage clamp recording 1–7 days after injection. "α1β1γ" and "α1β1δ" receptors were expressed by omitting cRNA for either the δ or γ subunit, respectively, from the usual α1βγδ cRNA injection mixture used to express wild-type muscle receptors (9, 10).

Voltage clamp recording was done as described previously (8). Briefly, oocytes were clamped at −70 mV with a two-electrode system and perfused with ND96 containing 1 μM atropine (to block any endogenous muscarinic acetylcholine receptors). ND96 consists of 96 mM NaCl, 2.0 mM KCl, 1.8 mM $CaCl_2$, 1.0 mM $MgCl_2$, 5 mM Hepes (pH 7.1–7.5). ACh-gated currents were elicited with 1-s pulses of 10 μM ACh (for *Torpedo* and mouse α1β1γ and α1β1δ nAChRs), 1 μM ACh (for wild-type muscle nAChRs), 300 μM (for α4β2, α3β2, and α3β4 nAChRs), and 1 mM ACh (for α7 nAChRs), applied at a frequency of 1/min, except for α4β2 receptors which were pulsed every 3 min to avoid desensitization. To elicit currents sufficient for recording a 10-fold higher concentration of ACh was necessary with α1β1γ and α1β1δ compared with wild-type nAChRs. When both ACh concentrations were tested on the wild-type muscle receptors the same toxin affinity was observed (data not shown). These results were expected given the short duration of ACh exposure during test pulses and the comparatively slow dissociation rate of the toxin. The ACh applied was approximately the lowest concentration required to elicit maximal current responses at each receptor subtype. For the muscle and *Torpedo* receptors, however, a submaximal concentration was chosen to allow the typically large current reponses to be voltage-clamped.

Toxins were applied in ND96 containing 1 μM atropine and 0.1 mg/ml bovine serum albumin. Exposure to each concentration of αA-EIVA or αA-EIVB was continued until the peak amplitudes of the ACh-gated currents reached a steady state. The average peak amplitude of at least four control responses recorded in the absence of toxin was used to normalize the response at each toxin concentration to obtain the "frac-

tional response." After application of toxin, the perfusion medium was switched back to ND96 with atropine. All kinetic and dose-response curves were generated using Prism software (GraphPad Software Inc., San Diego, CA). Dose-response curves were fit to the equation: fraction response = $1/(1 + ([\text{toxin}]/IC_{50})^{n_H})$ where n_H is the Hill coefficient.

Curve-fitting of Toxin Kinetics—It is assumed that the toxin (T) reversibly binds to its receptor site (*S*) according to the scheme,

$$T + S \underset{k_{off}}{\overset{k_{on}}{\Leftrightarrow}} TS$$

SCHEME 1

with forward and reverse rate constants k_{on} and k_{off}, respectively. It is also assumed that the amount of toxin greatly exceeds the number of sites, and thus the forward reaction follows pseudo-first order kinetics. We define $p(t)$ as the probability that a site is occupied by toxin at time t and $q(t)$ as the probability that the site is unoccupied; so $q(t) = (1 - p(t)$. If the system is initially at equilibrium, then when the concentration of toxin is perturbed to a new concentration $[T]$, the toxin occupancy of the site will relax to a new equilibrium value exponentially with a rate constant $k = (k_{on}[T] + k_{off})$ (see *e.g.* Ref. 6). Thus, p will follow a time course from its initial value $p(0)$ to its new equilibrium value $p(\infty)$ according to the equation

$$p(t) = [p(0) - p(\infty)]e^{-kt} + p(\infty) \quad \text{(Eq. 1)}$$

which rearranged yields

$$p(t) = p(0)e^{-kt} + p(\infty)[1 - e^{-kt}] \quad \text{(Eq. 2)}$$

Note that since $p(0)$ and $p(\infty)$ are equilibrium values before and after the toxin concentration was perturbed (say from $[T_0]$ to $[T]$), their values are given by the well-known relationship described by a rectangular hyperbola or binding isotherm, that is

$$p(0) = \frac{1}{1 + \frac{k_{off}}{k_{on}[T_0]}} \quad \text{(Eq. 3)}$$

and

$$p(\infty) = \frac{1}{1 + \frac{k_{off}}{k_{on}[T]}} \quad \text{(Eq. 4)}$$

It is also assumed that each receptor has N independent toxin-binding sites, and that occupancy of a single site is sufficient to inactivate the receptor. Then the probability that a receptor is active would be given by the probability that *none* of the sites on the receptor is occupied, and this in turn is given by the product of the probabilities of each site being *un*occupied; in other words, the fraction of receptors that are active, $FA(t)$, is given by $q^N(t)$ if the binding sites are kinetically equivalent. If sites are not equivalent, $FA(t)$ is the product of probabilities

$$FA(t) = \prod_{i=1}^{N} q_i(t) \quad \text{(Eq. 5)}$$

where q_i represents the probability that the ith site is unoccupied. Substituting the relationship in Equation 2 for $(1 - p(t))$ gives the following term for $q(t)$

$$q(t) = (1 - p(0)e^{-kt} - p(\infty)[1 - e^{-kt}]) \quad \text{(Eq. 6)}$$

which rearranged yields

$$q(t) = (1 + [p(\infty) - p(0)]e^{-kt} - p(\infty)) \quad \text{(Eq. 7)}$$

When k, $p(0)$, and $p(\infty)$ are replaced with their expanded versions given above, this yields

$$q(t) = \left(1 + \left[\frac{1}{1 + \frac{k_{off}}{k_{on}[T]}} - \frac{1}{1 + \frac{k_{off}}{k_{on}[T_0]}}\right]e^{-(k_{on}[T] + k_{off})t} - \frac{1}{1 + \frac{k_{off}}{k_{on}[T]}}\right) \quad \text{(Eq. 8)}$$

Thus, for nAChRs with two nonequivalent binding sites, where occupation of either site is sufficient to block receptor function, the fraction of active receptors is given by

$$FA(t) = \prod_{i=1}^{N} q_i(t) = q_1(t) \cdot q_2(t) \quad \text{(Eq. 9)}$$

with $q_i(t)$ specified by Equation 8 using the respective k_{on} and k_{off} for each site.

Note that when the initial concentration of toxin is zero (*i.e.* $[T_0] = 0$), then Equation 8 reduces to

$$q(t) = \left(1 - \left[\frac{1 - e^{-(k_{on}[T] + k_{off})t}}{1 + \frac{k_{off}}{k_{on}[T]}}\right]\right) \quad \text{(Eq. 10)}$$

Conversely, when the toxin is washed out (*i.e.* $[T] = 0$) following equilibration with a toxin concentration of $[T_0]$, Equation 8 reduces to

$$q(t) = \left(1 - \left[\frac{1}{1 + \frac{k_{off}}{k_{on}[T_0]}}\right]e^{-k_{off}t}\right) \quad \text{(Eq. 11)}$$

Our experiments monitored $FA(t)$ with pulses of ACh that produced brief responses (time to peak ~1 s). Thus, the receptors are exposed to ACh only for a relatively short time compared with the off-kinetics of the toxin ($1/k_{off}$) ~1 min), and ACh has only minimal opportunity to displace toxin from the receptors. We therefore assumed that the pulses of ACh did not perturb the binding of toxin to receptor. To simplify the curve-fitting of toxin wash-out, the binding isotherm $p(0)$, used to describe the initial conditions in Equation 11, was replaced by a variable, $1 - y_{min}$, and final conditions were described by a second variable, y_{max}, yielding the equation $y = (y_{max} - [1 - y_{min}]e^{-k_{off}t})^N$. The values for k_{off} were then used in Equation 10 to fit toxin wash-in curves and calculate k_{on} values.

Inhibition of ^{125}I-α-BTX Binding to Nicotinic Receptors on Intact BC$_3$H-1 Cells—Binding methods were as described previously (3). Briefly, BC$_3$H-1 cells were incubated in 250 μl of assay buffer (140 mM KCl, 25 mM HEPES, 5.4 mM NaCl, 1.8 mM $CaCl_2$, 1.7 mM $MgSO_4$, 0.06 mg/ml bovine serum albumin, pH 7.4) with or without αA-conotoxin EIVA. ^{125}I-α-BTX (10 μl, final concentration 20 nM) was then added, and the reaction was allowed to incubate for an additional 15 min. Cells were then washed twice with 2.0 ml of assay buffer to remove unbound ligands, and receptor-bound ^{125}I-α-BTX was removed from the wells with two 0.5-ml washes of 1% Triton X-100 in water and counted in a γ counter. Nonspecific binding was determined with cells previously exposed to 100 nM α-BTX for 30 min. The total density of ^{125}I-α-BTX binding sites was determined from a 60-min incubation in the absence of competing drug. Approximately 60–70% of the total specific ^{125}I-α-BTX binding sites were labeled by ^{125}I-BTX during the 15 min of the assays. All assays were performed at room temperature in triplicate.

RESULTS

Purification—Crude venom from *C. ermineus* obtained by milking snails was fractionated by HPLC. The elution pattern of two of the peptides paralytic to fish are shown in Fig. 2. These venom fractions were subfractionated until the peptides were purified to homogeneity. Disulfide bridges were reduced, and cysteines were alkylated prior to sequencing. Their amino acid sequences are as follows.

GCCGPYONAACHOCGCKVGROOYCDROSGG (A)

GCCGKYONAACHOCGCTVGROOYCDROSGG (B)

SEQUENCE 1

These sequences were confirmed by mass spectrometry (MH^+ = 3095.2 and 3099.1); these values are consistent with the peptides amidated at their C termini and with all of the Cys residues in disulfide linkages (calculated mass 3095.2 and 3099.2).

Chemical Synthesis of the Purified Peptides—Based on the putative sequences, the two peptides were synthesized by solid-state methods as described under "Experimental Procedures." The linear peptides were oxidized to form disulfide linkages. When air oxidation was used, the material corresponding to native peptide was not formed in high yield (data not shown). However, when glutathione oxidation was performed the major products corresponded to natural peptides by the criteria de-

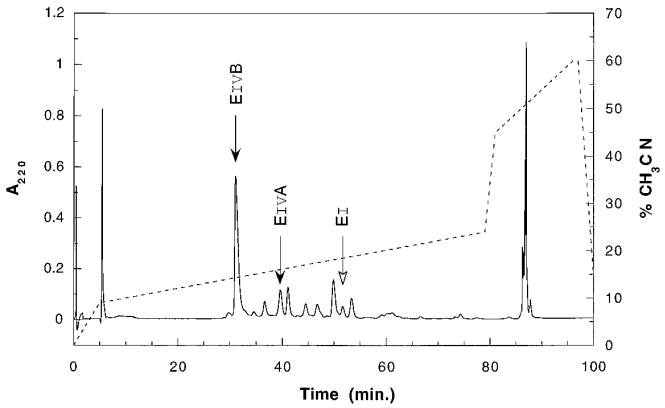

FIG. 2. **Purification of αA-conotoxins EIVA and EIVB from *C. ermineus* venom.** Buffer A = 0.1% trifluoroacetic acid; buffer B = 0.092% trifluoroacetic acid, 60% acetonitrile. Milked venom (see text) was applied to a semipreparative C_{18} Vydac column. The gradient program was 0–15% B for 5 min, 15–40% B for 74 min, 40–75% B for 3 min, followed by 75–100% B for 14 min; flow rate was 5 ml/min. The major components of the peptide absorbances indicated with *closed arrows* correspond to α-conotoxins EIVA and EIVB, respectively (eluting at 31.1 min and 39.6 min). These materials were purified to homogeneity using the semipreparative Vydac column described above with a gradient program beginning at 5–30% B for 75 min. Each of the major peaks was then subsequently run on an analytic Microsorb C_{18} column and eluted with a gradient program of 4–30% B for 75 min and flow rate of 1 ml/min (data not shown). The peptide absorbance indicated by the *open arrow* at 51.7 min corresponds to α-conotoxin EI, the isolation of which has been described previously (3).

scribed below (Fig. 3, *A* and *B*). These major products were purified to homogeneity. The cleavage of 100 mg of resin typically yielded 5–10 mg of biologically active peptide product.

When co-injected on HPLC the purified, chemically synthesized peptides co-eluted with the corresponding native peptide, as shown in Fig. 3, *C* and *D*. Mass spectrometric analysis showed that the molecular masses of synthetic peptides are consistent with the predicted sequences (MH^+ = 3095.2 and 3099.2; calculated mass 3095.19 and 3099.18). Furthermore, the paralytic activity of the synthetic peptides was quantitatively the same as that of the native peptides when injected into goldfish (data not shown). Thus, under glutathione oxidation conditions these peptides appear to form the disulfide linkages necessary to confer biological activity. Due to the limited availability of natural peptides, all subsequent experiments were performed with synthetic material.

Mechanism of Action of the Purified Peptides—The peptide sequences have considerable homology with that of αA-PIVA, which has been shown to be an antagonist of the nAChR at the neuromuscular junction. Given the strong homology between the peptides from *C. purpurascens* and *C. ermineus*, our initial hypothesis was that the *C. ermineus* peptides cause paralysis because they are also nAChR antagonists. To directly assess the functional effects of these peptides, electrophysiological experiments were carried out with cloned skeletal muscle nAChRs expressed in *Xenopus* oocytes. Fig. 4*A* shows the results obtained when the peptides were tested on oocytes expressing *Torpedo* nAChRs. It is clear that both peptides are potent inhibitors of ACh-gated currents under these conditions, with nearly identical IC_{50} values. Given these results and the structural homology to αA-PIVA, we designate these peptides as αA-conotoxins EIVA and EIVB.

α-MI is typical of many α-conotoxins from Indo-Pacific fish-hunting *Conus* venoms in that it prefers the α/δ over the α/γ interface of the mouse muscle nAChR (11, 12) and the α/γ over the α/δ (11–13) interface in the *Torpedo* electric organ nAChR. We compared the affinity of αA-EIVA for each interface by using receptors expressed in oocytes in which only cRNA for the

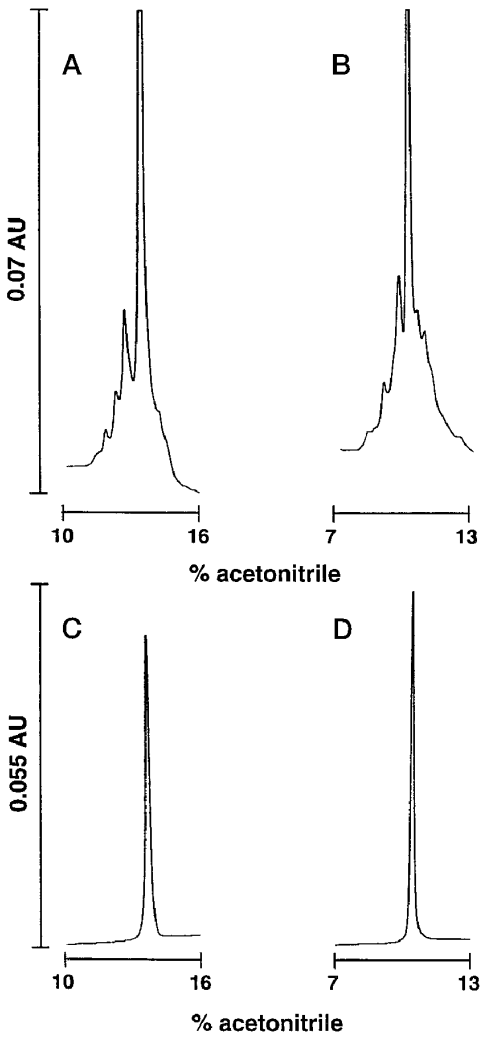

FIG. 3. **Chemical synthesis of αA-EIVA and αA-EIVB.** Disulfide bonds were formed in linear peptides by oxidation with glutathione (1 mM reduced, 0.5 mM oxidized, pH 7.5) for 24 h, yielding mixtures of isomers as shown by HPLC chromatograms in *A* for αA-EIVA and in *B* for αA-EIVB. The major peak in each reaction mixture was purified to homogeneity and found to co-elute using HPLC when co-injected with the natural peptides as shown in *C* for αA-EIVA and in *D* for αA-EIVB. HPLC-run conditions are detailed under *Peptide Synthesis* under "Experimental Procedures." Absorbance was measured at 220 nm.

mouse muscle α1, β1, δ or α1, β1, γ subunits was injected, forcing the formation of receptors with only α/δ or α/γ interfaces, respectively (9, 10). As a control, 10 nM α-bungarotoxin was tested on these receptors in duplicate experiments. α-Bungarotoxin blocked ~85% of the α1β1δ receptor response and ~92% of the α1β1γ receptor response after 15 min of exposure to toxin (data not shown). Fig. 4*B* shows the potency of αA-EIVA when tested on α1β1δγ nAChRs, termed wild-type receptors, and on the subunit-deficient variations of this receptor. These results differ markedly from those previously shown for α-MI, which prefers α1β1δ receptors with a discrimination index of 10^4 (14). The IC_{50} values of αA-EIVA for wild-type, α1β1δ, and α1β1γ receptors are almost identical. Thus, it appears that both the α1/δ and α1/γ interfaces are high affinity targets for αA-EIVA.

Toxin Kinetics—The wild-type mouse muscle nAChR is known to contain ACh binding sites at the α1/δ and α1/γ subunit interfaces (15), both of which must be occupied by agonist to activate the receptor. Receptors containing only α1β1δ or α1β1γ subunits have also been shown to contain two agonist binding sites which behave pharmacologically as a single class

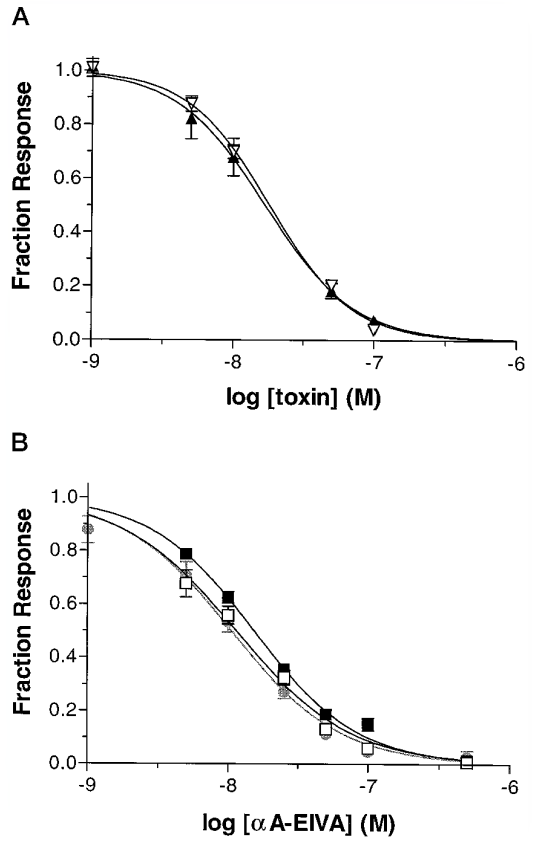

FIG. 4. **Dose-response curves for block of muscle nAChRs expressed in *Xenopus* oocytes by αA-EIVA and αA-EIVB.** *A*, block of *Torpedo* nAChRs by αA-EIVA (*open triangles*, IC_{50} 17 nM) and αA-EIVB (*closed triangles*, IC_{50} 18 nM). *B*, αA-EIVA block of mouse wild-type (*circles*, IC_{50} 11 nM), α1β1γ (*open squares*, IC_{50} 11 nM), and α1β1δ nAChRs (*closed squares*, IC_{50} 15 nM). *Error bars* are the S.E. (n = 3–7).

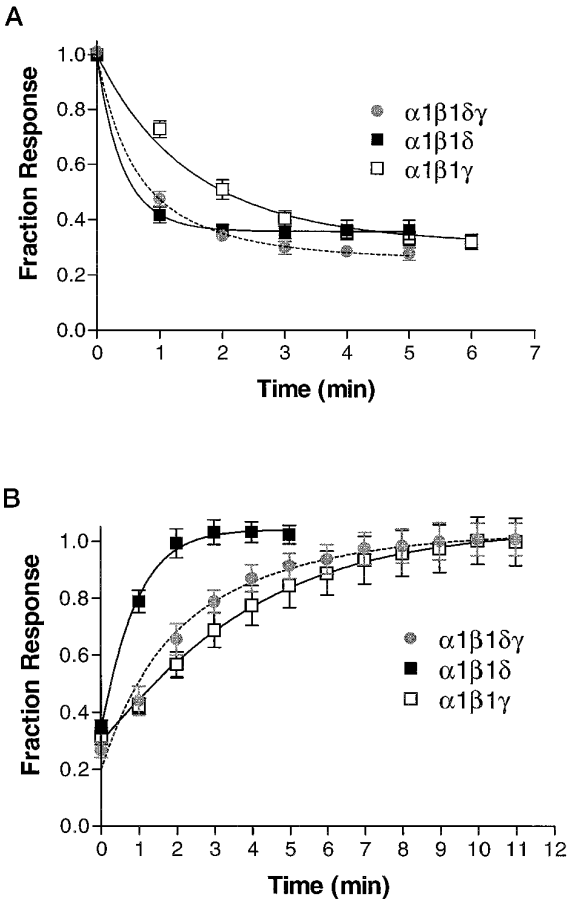

FIG. 5. **Kinetics of block by αA-EIVA of mouse muscle nAChRs expressed in *Xenopus* oocytes.** A 25 nM toxin solution was applied by perfusion at 1 ml/min, and currents were measured by pulsing with ACh at 1-min intervals. After an equilibrium blockade was achieved, toxin was washed out by perfusion of ND96 buffer solution. *A*, time course of block by toxin on wild-type (*circles*), α1β1γ (*open squares*, k_{on} = 0.94 × 10^7 ± 0.03 M^{-1} min^{-1}) and α1β1δ (*closed squares*, k_{on} = 3.37 × 10^7 ± 0.10 M^{-1} min^{-1}) nAChRs. The *dotted line* shows the curve fit to wild-type data by a model of two unequal binding sites using the k_{off} values for sites on the α1β1γ and α1β1δ nAChRs. Note that the k_{on} values for this curve, 1.65 × 10^7 ± 0.36 and 3.07 × 10^7 ± 0.91 M^{-1} min^{-1}, approximate those for the α1β1γ and α1β1δ receptors, respectively, with corresponding values within a 95% confidence interval of each other. *B*, recovery from block of wild-type (*circles*), α1β1γ (*open squares*, k_{off} = 0.30 ± 0.07 min^{-1}), and α1β1δ (*closed squares*, k_{off} = 1.26 ± 0.19 min^{-1}) nAChRs. A theoretical curve for the wild-type receptor (*dotted line*) was generated by a two-site binding model using k_{off} values for binding sites on the α1β1δ and α1β1γ receptors (R^2 = 0.82). All curves were fit as described under "Experimental Procedures." *Error bars* are the S.E. (α1β1δ, n = 2; α1β1γ, n = 3; wild-type, n = 5).

with respect to competitive antagonist binding (10). To calculate the rate constants k_{on} and k_{off} for the interaction of αA-EIVA with α1β1δ and α1β1γ receptors, we used the model with two equivalent competitive antagonist binding sites (at the two α1/δ or two α1/γ interfaces) in which binding to either site is sufficient to inhibit receptor function (10, 16). Since the wild-type receptor contains both an α1/δ and an α1/γ toxin binding site, the receptor should exhibit kinetics consistent with both sites. In fact, this is what was observed. Fig. 5 shows the time course of αA-EIVA block and recovery from block on α1β1δ, α1β1γ, and wild-type mouse muscle nAChRs. The parameters k_{on}, k_{off}, and K_d for these receptors are summarized in Table I. As shown in Fig. 5, use of the kinetic values calculated from α1β1δ and α1β1γ receptors provides a good description of block and recovery from block by αA-EIVA on the wild-type receptor.

The observed rates of both block and recovery from block by toxin was more rapid for α1β1δ *versus* α1β1γ receptors. For the wild-type receptor, the observed rate of toxin block was relatively fast, like that of the α1β1δ receptor. In contrast, the rate of recovery from toxin block for wild-type receptor was slower, comparable to that observed for the α1β1γ receptor. Thus, the kinetics of block of wild-type receptor appear to be dictated primarily by the faster toxin association rate of the α1/δ site, while the rate of recovery of receptor function following toxin wash-out is primarily influenced by the slower dissociation rate of the α1/γ site. This is the expected result if binding of toxin to a single agonist site is sufficient to block receptor function.

To investigate further the target specificity of αA-EIVA, we tested its activity on the α7 subtype of neuronal nAChRs. No detectable block of ACh-gated currents was observed in α7-expressing oocytes perfused with 1 μM αA-EIVA or upon exposure to 60 μM toxin in a static bath (data not shown). We also tested αA-EIVA on oocytes expressing α4β2, α3β2, or α3β4 nAChRs. 1 μM toxin (applied by perfusion) blocked α4β2 receptors ~25% but failed to block α3β2 or α3β4 nAChRs (n = 3).

To assess the mechanism of αA-EIVA action, binding experiments with radiolabeled α-bungarotoxin and muscle nAChR-expressing BC_3H-1 cells were carried out. The results of these experiments are shown in Fig. 6. In this assay, the αA-EIVA displaced all specific binding of ^{125}I-α-bungarotoxin to BC_3H-1 cells, consistent with the toxin being a competitive antagonist of the nAChR. In addition, the data are best fit by a dose-response curve for a single-site model. This is consistent with the oocyte studies indicating that αA-EIVA has nearly equal affinity for both the α/γ and α/δ sites.

TABLE I
Association and dissociation constants of αA-EIVA for nAChRs containing the indicated subunits

	k_{on} ($\times 10^7$)	k_{off}	Calculated site K_d[a]	Predicted IC_{50}[b]	Observed IC_{50}[b]
	$M^{-1}min^{-1}$	min^{-1}	nM	nM	nM
α1β1δ	3.37	1.26	37	15	15
α1β1γ	0.94	0.30	32	13	11

[a] The calculated K_d (k_{off}/k_{on}) is a measure of toxin affinity for a single binding site.

[b] The IC_{50} measures the functional block of receptor by toxin, presumably through binding at either of two pharmacologically equivalent binding sites present on a single receptor. The predicted IC_{50} was obtained from the calculated K_d using the equation: fractional response = $1/(1 + [\text{toxin}]/K_d)^2$. When [toxin] = IC_{50}, fractional response = 0.5, and this equation reduces to: $IC_{50} = 0.414 \cdot K_d$.

TABLE II
Subunit selectivity of toxin binding in mammalian nAChRs

	α1/δ	α1/γ	α7
α-MI	+	−	−
αA-EIVA	+	+	−
α-Bungarotoxin	+	+	+

DISCUSSION

The data presented above demonstrate the presence of two peptides from the venom of *C. ermineus*, αA-EIVA and αA-EIVB, which are competitive antagonists of nAChRs. αA-Conotoxin EIVA was examined in detail and has several notable functional features. First, unlike α-bungarotoxin, which has subnanomolar affinity for α7 nAChRs (17, 18), αA-EIVA does not block these receptors even at micromolar concentrations. In this regard, αA-EIVA behaves like α-conotoxins MI and GI, which potently target α1-containing, but not α7, nAChRs (18). Thus, *Conus* has evolved two independent structures that discriminate between α1 *versus* α7 receptors. However, like α-bungarotoxin, αA-EIVA has high affinity for both the α/δ and α/γ sites of the muscle subtype of nAChR as shown by both electrophysiological and radioligand binding experiments (although the peptide association and dissociation rates differ for each site). In contrast, α-conotoxins MI and GI are highly selective for the mouse muscle α/δ *versus* α/γ site (10^4-fold discrimination). These divergent specificities are summarized in Table II. The structural basis for these differences in ligand affinity is presently under investigation. In addition, a structural determination of αA-EIVA is almost complete.[3]

Sine *et al.* (14) have identified three critical residues in the δ nAChR subunit (Ser-36, Tyr-113, and Ile-178) which confer upon α-MI high α/δ *versus* α/γ affinity (14). When residues in the homologous positions of the γ subunit were mutated to contain these amino acids, mutant α1β1γ receptors had a high affinity for α-MI. The results of the present study suggest that αA-EIVA recognizes at least a partially different set of receptor residues from those recognized by α-MI, since αA-EIVA has a high affinity for both the α/δ and α/γ sites. Although it is possible that all of the contact residues for αA-EIVA binding are in the α subunit, it appears from the differences in kinetics of toxin binding to α1β1δ *versus* α1β1γ receptors that the δ and γ subunits also influence binding.

α-Bungarotoxin binds with high affinity and slow reversibility to both α/δ and α/γ sites in the mouse muscle nAChR (19, 20). Our experiments with radiolabeled α-bungarotoxin indicate that αA-EIVA can block all specific binding of α-bungarotoxin to BC_3H-1 cells in a concentration-dependent manner. The resulting dose-response curve is best fit by a single-site

[3] K.-H. Han, K. J. Hwang, S. K. Kim, W. R. Gray, B. M. Olivera, J. Rivier, and K. J. Shon, unpublished results.

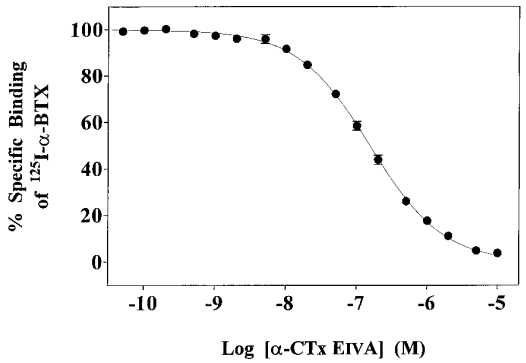

FIG. 6. **Inhibition of ^{125}I-α-BTX binding to nicotinic receptors on BC_3H-1 cells by αA-EIVA.** The data shown are the mean ± S.E. of four independent experiments. The IC_{50} and n_H were found to be 150 ± 10 nM and 0.85 ± 0.02, respectively. The data are fit best by a single-site competition model with a variable Hill coefficient (*solid line*) as determined by statistical comparison between a single-site and a two-site competition model ($p < 0.001$).

model. These results are consistent with those from oocyte experiments which indicate that αA-EIVA binds with nearly equal affinity at both an α/δ and α/γ site. However, αA-EIVA blocked α-bungarotoxin binding to mouse BC_3H-1 cells with an IC_{50} that was approximately 10-fold higher than that observed for αA-EIVA block of mouse muscle nAChRs expressed in oocytes. This difference is partly explained by the fact that αA-EIVA must occupy two binding sites on each receptor to completely block α-bungarotoxin binding, while block of functional response can occur by occupation of either site alone. This should result in an 2.4-fold difference between the functional block described by the IC_{50} in oocyte experiments and the IC_{50} observed by competition binding (see legend to Table I). Further differences in IC_{50} values between the experiments may be due to kinetic factors. In oocyte experiments, the binding equilibrium of αA-EIVA should not be affected appreciably by the brief applications (1-s pulses) of ACh due to the comparatively slow k_{off} of the toxin. In contrast, αA-EIVA has a much faster k_{off} than α-bungarotoxin. During the 15-min co-incubation of these toxins in the binding experiments, occupation of free binding sites by the essentially irreversible binding of α-bungarotoxin would be expected to shift the resultant dose-response curve of αA-EIVA toward a higher apparent IC_{50}.

αA-EIVA and αA-EIVB have similar sequences and may represent polymorphism in the *C. ermineus* population. Although these peptides are specifically targeted to the skeletal muscle subtype of the nAChR, they are broadly active in vertebrate systems; we demonstrated directly that they are antagonists when tested against skeletal muscle nAChRs in both elasmobranchs (*Torpedo* electroplax) and mammals (mouse).

In all fish-hunting cone snails, there appears to be at least one major peptide which is a competitive antagonist of skeletal muscle nAChRs; a summary of all such peptides from piscivorous *Conus* venoms which have been described thus far are shown in Table III. It is clear from the table that these peptides fall into two quite distinct families, the α-conotoxins and the αA-conotoxins. Before this report, only one αA-conotoxin had been described, αA-PVIA from *C. purpurascens* (2). The two peptides described here clearly exhibit homology to αA-PVIA, although they diverge substantially in sequence. As we noted previously, *C. purpurascens* and *C. ermineus* are the only fish-hunting cone snails known outside the Indo-Pacific region, and it is likely that they have long been isolated geographically from the major series of Indo-Pacific fish-hunting *Conus*. In all of the Indo-Pacific piscivorous species, an α-conotoxin is the major skeletal muscle nAChR antagonist.

C. ermineus is unusual in being the only *Conus* venom found

TABLE III
Competitive skeletal muscle nAChR antagonists from venoms of fish-hunting Conus

	Sequence	*Conus* species	Ref.
αA-EIVA	G**CC**GPYONAA**C**HO**C**G**C**KVGROOY**C**DROSGG[a]	*C. ermineus*	This work
αA-EIVB	G**CC**GKYONAA**C**HO**C**G**C**TVGROOY**C**DROSGG[a]	*C. ermineus*	This work
αA-PIVA	G**CC**GSYONAA**C**HO**C**S**C**KDROSY**C**GQ[a]	*C. purpurascens*	(2)
α-MI	GR**CC**HPA**C**GKNYS**C**[a]	*C. magus*	(22, 23)
α-GI	E**CC**NPA**C**GRHYS**C**[a]	*C. geographus*	(24)
α-GIA	E**CC**NPA**C**GRHYS**C**GK[a]	*C. geographus*	(24)
α-GII	E**CC**HPA**C**GKHFS**C**[a]	*C. geographus*	(24)
α-SIA	Y**CC**HPA**C**GKNFD**C**[a]	*C. striatus*	(25)
α-SI	I**CC**NPA**C**GPKYS**C**[a]	*C. striatus*	(26)
α-SII	G**CCC**NPA**C**GPNYG**C**GTS**C**S[b]	*C. striatus*	(27)
α-EI	RDO**CC**YHPT**C**NMSNPQI**C**[a]	*C. ermineus*	(3)

[a] Amidated C terminus; O, hydroxyproline.
[b] Free C terminus.

so far to contain both a major α-conotoxin as well as αA-conotoxins. The α-conotoxin described from *C. ermineus*, α-EI, is also divergent from those found in piscivorous Indo-Pacific species. However, it remains puzzling why this *Conus* species has both classes of competitive antagonists. At this time, we cannot distinguish between several hypotheses. Individual specimens of *C. ermineus* may express only the α- or only the αA-conotoxins at any one time, such as a seasonal variation in expression, or there may be polymorphism in the population. Since only pooled venom from many snails has been analyzed so far, we cannot eliminate these possibilities directly. Alternatively, it is possible that the α- and αA-peptides have intrinsically different functional targets, and that within an individual snail venom, both classes of peptides are expressed. For example, if the peptides have different efficacies at different types of teleost neuromuscular junctions or if the different fish prey of *C. ermineus* diverge significantly in their neuromuscular junction nAChRs, then it may be advantageous for the predator to have both conotoxin classes in its venom.

Conus species produce a remarkable variety of nicotinic receptor antagonists. The α-conotoxins with a "4/7" spacing (containing sequences of 4 and 7 consecutive non-cysteine amino acids, *i.e.*. CC----C-------C) are widely found in worm- and snail-hunting *Conus* species as well as some fish-hunting species (see Table III and Refs. 8 and 21).[4] These toxins target muscle nAChRs as well as neuronal subtypes and may represent the ancestral stem group of nAChR antagonists. The smaller peptides with "3/5" spacing, produced by Indo-Pacific species, and the larger αA-conotoxins may represent separate evolutionary lineages for targeting vertebrate muscle nAChRs.

Acknowledgments—Mass spectrometry was performed by A. Gray Craig of the Salk Institute, La Jolla, CA. We thank Lourdes J. Cruz and Christopher Hopkins for providing the milked venom.

[4] R. Jacobsen, D. Yoshikami, M. Ellison, J. Martinez, W. R. Gray, G. E. Cartier, K.-J. Shon, D. R. Groebe, S. N. Abramson, B. M. Olivera, and J. M. McIntosh, unpublished data.

REFERENCES

1. Myers, R. A., Cruz, L. J., Rivier, J., and Olivera, B. M. (1993) *Chem. Rev.* **93,** 1923–1936
2. Hopkins, C., Grilley, M., Miller, C., Shon, K.-J., Cruz, L. J., Gray, W. R., Dykert, J., Rivier, J., Yoshikami, D., and Olivera, B. M. (1995) *J. Biol. Chem.* **270,** 22361–22367
3. Martinez, J. S., Olivera, B. M., Gray, W. R., Craig, A. G., Groebe, D. R., Abramson, S. N., and McIntosh, J. M. (1995) *Biochemistry* **34,** 14519–14526
4. Guddat, L. W., Martin, J. A., Shan, L., Edmundson, A. B., and Gray, W. R. (1996) *Biochemistry* **35,** 11329–11335
5. Hu, S.-H., Gehrmann, J., Guddat, L. W., Alewood, P. F., Craik, D. J., and Martin, J. L. (1996) *Structure* **4,** 417–423
6. Hille, B. (1992) *Ionic Channels of Excitable Membranes*, 2nd Ed., Sinauer Associates, Inc., Sunderland, MA
7. Shon, K.-J., Hasson, A., Spira, M. E., Cruz, L. J., Gray, W. R., and Olivera, B. M. (1994) *Biochemistry* **33,** 11420–11425
8. Cartier, G. E., Yoshikami, D., Gray, W. R., Luo, S., Olivera, B. M., and McIntosh, J. M. (1996) *J. Biol. Chem.* **271,** 7522–7528
9. Charnet, P., Labarca, C., and Lester, H. A. (1991) *Mol. Pharmacol.* **41,** 708–717
10. Sine, S. M., and Claudio, T. (1991) *J. Biol. Chem.* **266,** 19369–19377
11. Kreienkamp, H.-J., Sine, S. M., Maeda, R. K., and Taylor, P. (1994) *J. Biol. Chem.* **269,** 8108–8114
12. Groebe, D. R., Dumm, J. M., Levitan, E. S., and Abramson, S. N. (1995) *Mol. Pharmacol.* **48,** 105–111
13. Hann, R. M., Pagán, O. R., and Eterovic, V. A. (1994) *Biochemistry* **33,** 14058–14063
14. Sine, S. M., Kreienkamp, H.-J., Bren, N., Maeda, R., and Taylor, P. (1995) *Neuron* **15,** 205–211
15. Blount, P., and Merlie, J. P. (1989) *Neuron* **3,** 349–357
16. Taylor, P., Brown, R. D., and Johnson, D. A. (1983) *Curr. Top. Membr. Transp.* **18,** 407–444
17. Séguéla, P., Wadiche, J., Dineley-Miller, K., Dani, J. A., and Patrick, J. W. (1993) *J. Neurosci.* **13,** 596–604
18. Johnson, D. S., Martinez, J., Elgoyhen, A. B., Heinemann, S. S., and McIntosh, J. M. (1995) *Mol. Pharmacol.* **48,** 194–199
19. Sine, S. M., and Claudio, T. (1991) *J. Biol. Chem.* **266,** 13679–13689
20. Groebe, D. R., and Abramson, S. N. (1995) *J. Biol. Chem.* **270,** 281–286
21. Fainzilber, M., Hasson, A., Oren, R., Burlingame, A. L., Gordon, D., Spira, M. E., and Zlotkin, E. (1994) *Biochemistry* **33,** 9523–9529
22. McIntosh, M., Cruz, L. J., Hunkapiller, M. W., Gray, W. R., and Olivera, B. M. (1982) *Arch. Biochem. Biophys.* **218,** 329–334
23. Gray, W. R., Rivier, J. E., Galyean, R., Cruz, L. J., and Olivera, B. M. (1983) *J. Biol. Chem.* **258,** 12247–12251
24. Gray, W. R., Luque, A., Olivera, B. M., Barrett, J., and Cruz, L. J. (1981) *J. Biol. Chem.* **256,** 4734–4740
25. Myers, R. A., Zafaralla, G. C., Gray, W. R., Abbott, J., Cruz, L. J., and Olivera, B. M. (1991) *Biochemistry* **30,** 9370–9377
26. Zafaralla, G. C., Ramilo, C., Gray, W. R., Karlstrom, R., Olivera, B. M., and Cruz, L. J. (1988) *Biochemistry* **27,** 7102–7105
27. Ramilo, C. A., Zafaralla, G. C., Nadasdi, L., Hammerland, L. G., Yoshikami, D., Gray, W. R., Kristipati, R., Ramachandran, J., Miljanich, G., Olivera, B. M., and Cruz, L. J. (1992) *Biochemistry* **31,** 9919–9926